Automated description of colours in polarized-light surface microscopy images of melanocytic lesions

Giovanni Pellacani[a], Costantino Grana[b] and Stefania Seidenari[a]

The aim of this study was to develop a computerized method for the identification and description of colour areas in melanocytic lesion images based on an approach mimicking the human perception of colours. A colour palette comprising six colour groups (black, dark brown, light brown, blue-grey, red and white) was created by selecting single colour components within melanocytic lesion images acquired using a digital videomicroscope, and was implemented in the image analysis program. For each colour region, the area, the distance from the lesion centroid, the spread, the colour area distribution in the internal and the external part of the lesion, and asymmetries were assessed on 604 melanocytic lesion images in our image database. Black, white and blue-grey colour areas were detected more frequently in melanomas compared with naevi. Moreover, significant differences in colour descriptors were observed for each colour group, showing that colour areas are more unevenly distributed in melanomas compared with naevi. Using a discriminant analysis approach, the extension of dark, white and blue-grey areas and some descriptors of the distribution of the colour areas were identified as the most relevant colour parameters for differentiating between benign and malignant lesions. In conclusion, our automatic procedure breaks down the image into the colour areas used in the clinical examination process, and also supplies a description of their extension and distribution, with parameters that correlate with the clinical concepts of regularity and homogeneity. *Melanoma Res* 14:125–130

Melanoma Research 2004, **14:**125–130

Keywords: Melanoma, image analysis, automated diagnosis, epiluminescence, dermatoscopy, colours, computer

Departments of [a]Dermatology and [b]Computer Engineering, University of Modena and Reggio Emila, Italy.

Sponsorship: This study was partially supported by MIUR (Ministero dell'Istruzione dell'Università e della Ricerca) grant number 2001068929.

Correspondence and requests for reprints to Stefania Seidenari, Department of Dermatology, University of Modena and Reggio Emilia, 41100 Modena, Italy.
Tel: +39 59 4222464; fax: +39 59 4224271;
e-mail: seidenar@unimo.it

Received 12 June 2003 **Accepted** 1 January 2004

Introduction

Early melanoma diagnosis is an important goal for dermatologists. Skin surface microscopy [1,2] in association with a reference terminology [3,4] improves the diagnostic accuracy for malignant melanoma (MM) [5], in spite of unavoidable subjectivity and variability in the interpretation of dermoscopic images [3,6]. To overcome these problems, programs for image analysis, enabling the numerical description of the morphology of pigmented skin lesion images, have been recently developed. Some of these have provided reproducible quantification of lesion features and can act as an aid for clinical diagnosis [7–16]. In these programs, colours are described by means of numerical data calculated from different colour channels, such as the average value and standard deviation of red, green and blue (RGB) [7,8,10,11,17] or the hue, saturation and value (HSV) [12,18]. However, these descriptors are unable to describe colours as the human eye perceives them.

Recently we described a method for the evaluation of colours in melanocytic lesion (ML) images based on an approach which is similar to the human perception of colours [19]. A colour palette comprising six colour groups (black, dark brown, light brown, blue-grey, red and white) was interactively created by selecting single colour components inside ML images acquired using a digital videomicroscope, and was implemented in the image analysis program. Colours were then assessed by the computer program on 331 ML images in our image database, and the results were compared with evaluation of the lesion colours performed by a clinician. An excellent concordance between human and machine evaluation of the number and type of colours was obtained with this method. Some colours were more frequently found in MMs than in naevi by both the clinician and the computer. Furthermore, MM images presented a higher number of colours than naevus images.

Not only do the type and number of colours vary between benign and malignant ML images, there is also a difference in the colour distribution, which strongly influences the asymmetry of the lesion. In this study a numerical description of the aspect and distribution of different colour areas in naevi and MMs was provided. The most relevant colour parameters for MM diagnosis were identified by testing them on a group of benign and

0960-8931 DOI: 10.1097/01.cmr.0000124659.76546.40

malignant ML images, in order to evaluate the efficacy of descriptors in distinguishing between the two groups.

Materials and methods

Image database

A total of 604 images of pigmented skin lesions comprising 113 MMs and 491 melanocytic naevi were studied. Images were acquired using a digital videomicroscope (VMS-110A; Scalar Mitsubishi, Tama-shi, Tokyo, Japan) with a 20-fold magnification, enabling the whole lesion to be included in the monitor area. This instrument has been described elsewhere [11]. The images were digitized using a Matrox Orion frameboard and stored by an image acquisition program (VideoCap 8.09, DS-Medica, Milan, Italy) that runs under Microsoft Windows. The camera system was calibrated monthly on a set of colour patches with known colour properties (Color Checker, Gretag Machbet, New Windsor, NY, USA). The resulting colour profile was adjusted on a white test patch between each patient examination, according to the method proposed by Haeghen and co-workers [20] with slight modifications. Contrast enhancement was applied to the skin colour volume of the standard RGB (sRGB) colour space before quantification, obtaining a finer step description of each colour channel. This modified colour space will be named $R^*G^*B^*$. The digitized images offer a spatial resolution of 768×576 pixels and a resolution of 16 million colours.

Image analysis program

The image analysis program was created using MS visual C++ 6.0 for both palette generation and colour region detection and elaboration.

Interactive creation of the colour palette

Our palette was created from a database comprising 30 pigmented skin lesion images unequivocally showing black, dark brown, light brown, red, white and blue-grey colour components, and comprised these six colour groups in 98 colour patches corresponding to the minimum number of colour shades permitting a sufficiently accurate description of single colours.

Colour region detection

The resulting palette was used to extract the colour regions from the images. Each pixel of the image was assigned to the colour patch that minimized its Euclidean distance in the R*G*B* colour space. After assigning all pixels to their corresponding patches, those belonging to the same group were merged together to form the region corresponding to that particular colour (Fig. 1). The method for palette creation and colour region detection has been described in detail elsewhere [19].

Colour region parameters

For each colour region, a set of parameters was extracted in order to numerically describe the colour region properties. After detection of the lesion border [21] and extraction of reference geometrical measures such as the centroid and main inertia axes according to standard algorithms, the lesion was divided into two zones corresponding to different semantic parts. The internal zone corresponded to 80% of the distance between the centroid and the furthest border point along the same direction. The remaining part of the lesion belonged to the external zone. For each colour region, the area, distance from the centroid, spread, colour area distribution in the internal and the external part of the lesion, and asymmetries were calculated. Mathematical and clinical descriptions of these parameters are given in Table 1.

Fig. 1

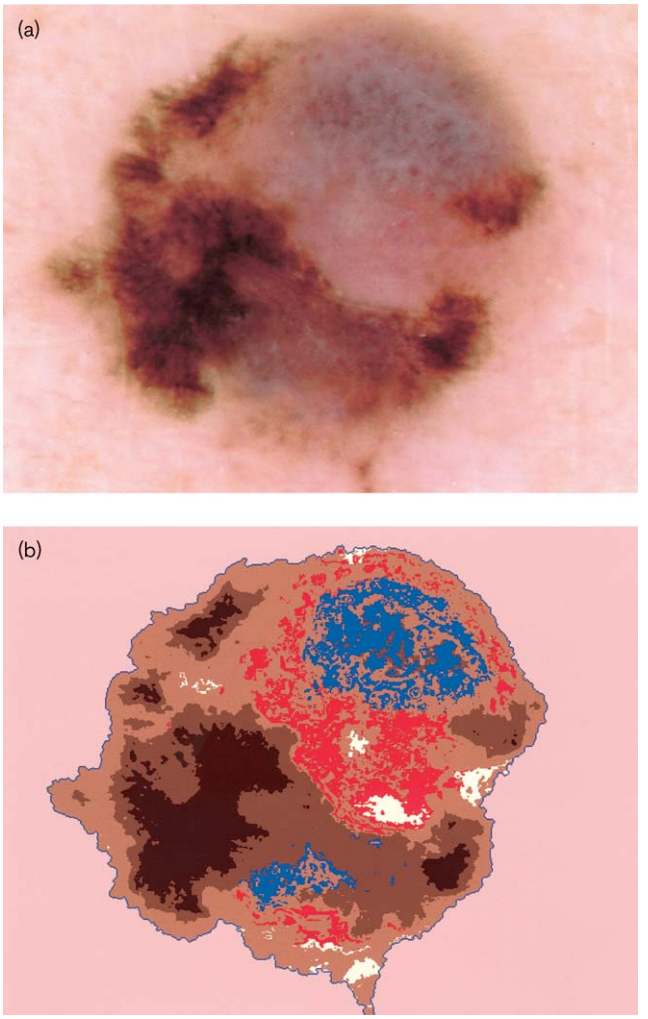

Example of colour area identification in a melanoma: (a) 20-fold videomicroscopic image; (b) corresponding image with highlighted colour areas.

Table 1 Mathematical and clinical descriptions of the parameters used

Parameter	Range	Mathematical description	Clinical description
AREA	0–1	Number of pixels composing the colour area divided by the number of pixels corresponding to the lesion area	Extension of the colour area
DIST-C	0–1	Distance between the colour region centroid and the lesion centroid, divided by the length of the major axis	Colour distribution balance
SPRE	1–∞	First invariant obtained by the sum of the second-order moments with respect to the lesion centroid, divided by the squared area	Colour region compactness
PERC-INT	0–1	Number of pixels of the colour region in the internal zone divided by the total number of pixels of that colour area	Colour distribution
PERC-EXT	0–1	Number of pixels of the colour region in the internal zone divided by the total number of pixels of that colour area	Colour distribution
ASYM-MAX	0–1	Absolute difference between the number of points on each side of the main axes divided by the total number of pixels of that colour area (higher value)	Asymmetry of the colour distribution
ASYM-MIN	0–1	Absolute difference between the number of points on each side of the main axes divided by the total number of pixels of that colour area (lower value)	Asymmetry of the colour distribution
%	0–100	Presence/absence	Percentage of lesions with the colour area

Statistics

The SPSS statistical package (release 10.0.06, 1999, SPSS Inc., Chicago, Illinois, USA) was used for statistical analysis. The mean and SD of the colour parameters were calculated both for MMs and naevi. Differences between naevus and MM values were evaluated using the Mann–Whitney *U*-test for independent samples. A P value < 0.01 was considered to be significant.

In order to validate our method for colour description and its efficacy in distinguishing between benign and malignant MLs, the study population was randomly divided into a training set comprising 192 lesions (42 melanomas and 150 melanocytic naevi) and a test set comprising 412 lesions (71 melanomas and 341 melanocytic naevi). Values referring to parameters belonging to the training set underwent elaboration by means of multivariate discriminant analysis, and the variables used for distinction among the groups were identified. A linear combination of the independent variables was formed and a score (D), representing the basis for assigning cases to groups, was obtained for all the lesions.

Receiver operating characteristic (ROC) analysis was performed to investigate the sensitivity and specificity of the discriminant equation for image classification [22]. Sensitivity, specificity and diagnostic accuracy, estimated by the ratio between the percentage of the sum of true positives and true negatives, were calculated for each threshold (D) value. The area under the curve (AUC), which represents an index of the overall discriminant power, was calculated using the non-parametric trapezoidal method. To estimate melanoma risk, calculation of the odds ratio (OR) and 95% confidence interval (95% CI) was performed, using the D score value with the best diagnostic accuracy as the threshold value.

Results

The mean and SD of the parameters calculated for each colour group are listed in Table 2. Black colour areas were detected more frequently in MMs than in naevi (82.3 versus 61.9%). Black areas, when present, were larger and more unbalanced in melanomas compared with naevi, as shown by greater AREA and DIST-C values. In melanomas, 11.7% of the black area was located in the external zone, whereas in naevi the external zone appeared to be only minimally involved.

Almost all the lesions examined had dark brown areas, which were less represented and more asymmetrically and non-homogeneously distributed in melanomas, as demonstrated by lower AREA and greater DIST-C, SPRE, ASYM-MAX and ASYM-MIN values. In naevi the dark brown area was distributed predominantly in the internal portion of the lesion, whereas in melanomas it widely involved the external zone of the lesion.

Light brown areas were present in 64.6 and 75.7% of MMs and naevi, respectively. These were mainly found in the external zone of the lesion in both cases, but in MMs they were smaller and more irregularly distributed, as demonstrated by lower AREA and greater ASYM-MAX and ASYM-MIN values.

Red colour areas were detected equally in MMs and naevi (37.1 and 38.9%, respectively) and no differences in their extension were found, but in MMs they prevailed in the internal zone, and were unbalanced (greater DIST-C) and irregularly distributed (greater ASYM-MIN and ASYM-MAX).

White areas were more frequently identified in melanomas (26.5%) compared with naevi (13.8%) and were more unevenly distributed (greater DIST-C and ASYM-MAX values).

Blue-grey areas were more frequently detected in malignant lesions compared with benign ones (45.1% in MMs versus 25.6% in naevi) and were larger in the former.

Table 2 Mean ± SD of the parameters calculated for each colour group on 604 pigmented skin lesion images comprising 113 melanomas and 491 melanocytic naevi

Parameter	Black		Dark brown		Light brown		Red		White		Blue-grey	
	MM	Naevus	MM	Naevus	MM	Naevus	MM	Naevus	MM	Naevus	MM	Naevus
AREA	0.330 ± 0.276*	0.174 ± 0.217	0.264 ± 0.154*	0.339 ± 0.166	0.291 ± 0.278*	0.376 ± 0.2274	0.026 ± 0.048	0.028 ± 0.057	0.020 ± 0.045*	0.012 ± 0.040	0.015 ± 0.026*	0.006 ± 0.014
DIST-C	0.082 ± 0.071*	0.054 ± 0.047	0.074 ± 0.059*	0.039 ± 0.041	0.068 ± 0.055*	0.029 ± 0.026	0.122 ± 0.060*	0.057 ± 0.034	0.135 ± 0.080*	0.082 ± 0.047	0.079 ± 0.050	0.062 ± 0.035
SPRE	0.544 ± 0.768*	0.596 ± 0.913	0.801 ± 0.558*	0.566 ± 0.815	0.693 ± 0.477	0.570 ± 0.319	4.640 ± 3.895*	4.961 ± 3.586	4.371 ± 3.197*	4.534 ± 2.884	8.125 ± 4.663	10.349 ± 5.668
PERC-INT	0.883 ± 0.094*	0.967 ± 0.051	0.644 ± 0.236*	0.804 ± 0.213	0.419 ± 0.164	0.390 ± 0.180	0.608 ± 0.155*	0.466 ± 0.225	0.480 ± 0.223*	0.269 ± 0.150	0.669 ± 0.222	0.712 ± 0.210
PERC-EXT	0.116 ± 0.094*	0.032 ± 0.051	0.356 ± 0.236*	0.196 ± 0.213	0.581 ± 0.164*	0.610 ± 0.180	0.391 ± 0.155*	0.534 ± 0.225	0.520 ± 0.223*	0.731 ± 0.150	0.301 ± 0.222	0.288 ± 0.210
ASYM-MAX	0.348 ± 0.283	0.288 ± 0.246	0.283 ± 0.226*	0.176 ± 0.178	0.238 ± 0.180*	0.107 ± 0.085	0.455 ± 0.228*	0.207 ± 0.122	0.494 ± 0.259*	0.259 ± 0.168	0.306 ± 0.207	0.242 ± 0.144
ASYM-MIN	0.145 ± 0.172	0.124 ± 0.161	0.109 ± 0.114*	0.070 ± 0.096	0.094 ± 0.085*	0.043 ± 0.047	0.203 ± 0.171*	0.087 ± 0.076	0.167 ± 0.197	0.111 ± 0.138	0.119 ± 0.107	0.111 ± 0.109
%	83.3%*	61.9%	92.0%	95.1%	64.6%	75.8%	37.2%	38.9%	26.5%*	13.8%	45.1%*	25.7%

*Statistically significant.

Discriminant analysis

The equation developed for the classification into MMs and naevi was as follows:

$$\begin{aligned} D = &\text{black}\,[(\text{AREA})\times 1.095 + (\text{DIST-C})\times 1.611 \\ &+ (\text{PERC-EXT})\times 4.610] \\ &+ \text{dark brown}\,[(\text{DIST-C}) \\ &\times 19.269 + (\text{PERC-EXT})\times 0.569 \\ &+ (\text{ASYM-MAX})\times -3.264] \\ &+ \text{light brown}\,[(\text{DIST-C})\times 31.835 \\ &+ (\text{ASYM-MAX})\times -6.344] \\ &+ \text{red}\,[(\text{DIST-C})\times 8.335 + (\text{ASYM-MAX}) \\ &\times -1.994] + \text{white}\,[(\text{AREA})\times -2.589 \\ &+ (\text{PERC-INT})\times 4.614] + \text{grey-blue}\,[(\text{AREA}) \\ &\times -2.589 + (\text{SPRE})\times -0.026 \\ &+ (\text{ASYM-MAX})\times 3.767] - 1.6 \end{aligned}$$

The mean and SD of the D values were 1.243 ± 1.704 for melanomas and −0.542 ± 0.887 for naevi.

Figure 2 shows the ROC curve for the D scores for distinction between melanomas and naevi. The AUC value was 0.830. Table 3 shows the sensitivity, specificity and diagnostic accuracy values obtained for different D score cut-off points. For a D score equal to 0, corresponding to the best diagnostic accuracy value (77.7%), a sensitivity of 77.9% and a specificity of 77.6% were obtained. According to the OR calculation,

Fig. 2

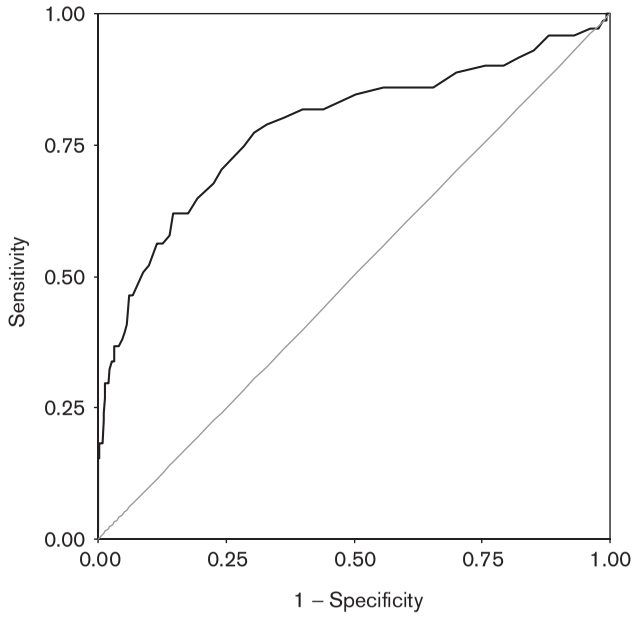

ROC curve for D scores in the detection of melanoma (AUC = 0.830).

Table 3 Sensitivity, specificity and diagnostic accuracy values at various D score cut-off points for the detection of melanoma

D score cut-off point	Sensitivity (%)	Specificity (%)	Diagnostic accuracy (%)
−3.40	100	0	50.0
−1.70	97.3	6.3	51.8
−1.40	95.6	15.5	55.5
−1.30	93.8	18.5	56.2
−1.00	91.2	33.2	62.2
−0.85	90.3	40.1	65.2
−0.70	89.4	49.1	69.2
−0.45	85.8	61.5	73.7
−0.20	81.4	70.3	75.8
0.00	**77.9**	**77.4**	**77.6**
0.10	73.5	80.0	76.7
0.20	70.8	83.1	76.9
0.50	62.8	88.2	75.5
0.65	58.4	90.4	74.4
0.80	53.1	92.9	73.0
1.00	48.7	94.5	71.6
1.30	42.5	95.9	69.2
2.00	33.6	97.8	65.7
7.50	0	100	50.0

The numbers in bold indicate the best diagnostic accuracy.

a D score greater than 0 was highly predictive for melanoma (OR = 12.19, 95% CI 7.45–19.95).

Discussion

Colour identification is an important step in the clinical diagnosis of pigmented skin lesions by means of epiluminescence microscopy [23]. The colours of the lesions are usually described in terms of six main colour groups: black, dark brown, light brown, red, white and blue-grey. Some colours and hues are of greater clinical relevance than others. Blue-grey areas, pink or white regions and irregularly distributed black blotches are suggestive of melanoma [2,24–26], but the identification of these structures is not completely reproducible [4,6]. Semiquantitative methods based on pattern analysis have been introduced in order to improve the reproducibility of diagnostic judgement. With the ABCD rule for dermatoscopy, the 'C' score, attributed on the basis of the total number of colours of the lesion, contributes approximately 30% of the final score [27]. Both using the Menzies' method [28] and the new seven-point check list [29], the presence of some colour structures, such as blue-grey areas and regression or scar-like depigmentation, appears to be relevant for melanoma diagnosis.

Systems for the analysis of pigmented skin lesion images have so far employed certain colour parameters for the automated diagnosis of melanomas [7–18]. Colours are mainly evaluated in terms of their RGB [7,8,10,11,17] or HSV [12,18] components, obtaining information on the overall coloration of the lesion but not enabling the identification of precise colour areas. Applying the median cut algorithm, Ganster *et al.* [16] selected 15 colours from a subset of characteristic lesions and calculated the number of colours and their extension inside benign and malignant lesions. Although these colour parameters appear to be useful for the automated diagnosis of melanoma, they do not reproduce the human perception process. We recently created a method for the identification of colour areas closely following the clinical evaluation procedure [19]. In this study we propose a procedure for colour area description to be employed by systems for computer-aided diagnosis. Descriptors of colour area size and distribution were tested on a dataset consisting of MMs and naevi using the discriminant analysis approach. This method enabled the identification and selection of the colour parameters most useful for distinguishing between MMs and naevi and, combining them in a linear equation, generated a score for each lesion for attribution to the diagnostic group, enabling discrimination between MMs and naevi with a diagnostic accuracy of 77.7%.

Colour area size and distribution characteristics for MMs and naevi were identified. In particular, the extension, asymmetry and the non-homogeneity of the black areas were typical for melanomas, whereas a regular distribution of dark areas (black or dark brown), usually located centrally and surrounded by a homogeneous light brown ring, was more frequently found in naevi. In previous studies based on dermoscopic images, the presence of red areas, corresponding to increased vascularization, appeared to be characteristic for melanoma [3,29,30]. In contrast, in our lesions recorded using a polarized-light videomicroscope, the red component was observed in the same proportion in the two groups owing to the effects of the polarizing filter and the blood stasis caused by placing the spacer-ring on the skin [31,32]. However, whereas in naevi the red colour component was homogeneously distributed over the whole lesion area, in MMs the red areas were asymmetrically distributed, as shown by greater asymmetry values and a higher distance from the centroid. White colour areas appeared characteristic of malignant lesions, and were larger and more unevenly distributed than in naevi. Blue-grey areas were observed more frequently in MMs compared with naevi (45.1 versus 25.7%, respectively) and were also more extended (greater AREA) and aggregated (lower SPRE) in the former.

Parameters used by programs for image analysis usually derive from mathematical definitions not easily intelligible to clinicians and that do not correspond to the human perception of characteristic clinical aspects. Our system not only resolves the image into colour areas according to the usually employed clinical examination process, but also supplies a description of their extension and distribution with parameters correlated to the clinical concepts of regularity and homogeneity.

Although the colour palette used in this study is strictly applicable only to pigmented skin lesions acquired with

the same instrument and technique, the method employed for the generation of the colour palette and colour groups makes this system adaptable to images generated by different acquisition methods.

References

1 Pehamberger H, Steiner A, Wolff K. *In vivo* epiluminescence microscopy of pigmented skin lesions. I. Pattern analysis of pigmented skin lesions. *J Am Acad Dermatol* 1987; **17**:571–583.

2 Kenet RO, Kang S, Kenet BJ, Fitzpatrick TB, Sober AJ, Barnhill RL. Clinical diagnosis of pigmented lesions using digital epiluminescence microscopy. *Arch Dermatol* 1993; **129**:157–174.

3 Bahmer FA, Fritsch P, Kreusch J, Pehamberger H, Rohrer C, Schindera I, *et al.* Terminology in surface microscopy. *J Am Acad Dermatol* 1990; **23**:1159–1162.

4 Argenziano G, Soyer HP, Chimenti S, Talamini R, Corona R, Sera F, *et al.* Dermoscopy of pigmented skin lesions: results of a consensus meeting via the internet. *J Am Acad Dermatol* 2003; **48**:679–693.

5 Bufounta ML, Beauchet A, Aegerter P, Saiag P. Is dermoscopy (epiluminescence microscopy) useful for the diagnosis of melanoma? *Arch Dermatol* 2001; **137**:1343–1350.

6 Stanganelli I, Burroni M, Rafanelli S, Bucchi L. Intraobserver agreement in interpretation of digital epiluminescence microscopy. *J Am Acad Dermatol* 1995; **33**:584–589.

7 Schindewolf T, Stolz W, Albert R, Abmayr W, Harms H. Classification of melanocytic lesions with color and texture analysis using digital image processing. *Anal Quant Cytol Histol* 1993; **15**:1–11.

8 Green AC, Martin NG, Pfitzner J, O'Rourke M, Knight N. Computer image analysis in the diagnosis of melanoma. *J Am Acad Dermatol* 1994; **31**: 958–964.

9 Hall PN, Claridge E, Morris Smith JD. Computer screening for early detection of melanoma – is there a future? *Br J Dermatol* 1995; **132**: 325–338.

10 Gutkowicz-Krusin D, Elbaum M, Szwaykowski P, Kopf AW. Can early malignant melanoma be differentiated from atypical melanocytic nevus by *in vivo* techniques? Part II. Automatic machine vision classification. *Skin Res Technol* 1997; **3**:15–22.

11 Seidenari S, Pellacani G, Pepe P. Digital videomicroscopy improves diagnostic accuracy for melanoma. *J Am Acad Dermatol* 1998; **39**: 175–181.

12 Binder M, Kittler H, Seeber A, Steiner A, Pehamberger H, Wolff K. Epiluminescence microscopy-based classification of pigmented skin lesions using computerized image analysis and an artificial neural network. *Melanoma Res* 1998; **8**:261–266.

13 Seidenari S, Pellacani G, Giannetti A. Digital videomicroscopy and image analysis with automatic classification for detection of thin melanomas. *Melanoma Res* 1999; **9**:163–171.

14 Andreassi L, Perotti R, Rubegni P, Burroni M, Cevenini G, Biagioli M, *et al.* Digital dermoscopy analysis for the differentiation of atypical nevi and early melanoma. *Arch Dermatol* 1999; **135**:1459–1465.

15 Pellacani G, Martini M, Seidenari S. Digital videomicroscopy with image analysis and automatic classification as an aid for diagnosis of Spitz nevus. *Skin Res Technol* 1999; **5**:266–272.

16 Ganster H, Pinz A, Rohrer R, Wildling E, Binder M, Kittler H. Automated melanoma recognition. *IEEE Trans Med Imaging* 2001; **20**: 233–239.

17 Aitken JF, Pfitzner J, Battistutta D, O'Rourke PK, Green AC, Martin NG. Reliability of computer image analysis of pigmented skin lesions of Australian adolescents. *Cancer* 1996; **78**:252–257.

18 Cascinelli N, Ferrario M, Bufalino R, Zurrida S, Galimberti V, Mascheroni L, *et al.* Results obtained by using a computerized image analysis system designed as an aid to diagnosis of cutaneous melanoma. *Melanoma Res* 1992; **2**:163–170.

19 Seidenari S, Pellacani G, Grana C. Computer description of colours in dermoscopic melanocytic lesion images reproducing clinical assessment. *Br J Dermatol* 2003; **149**: 523–529.

20 Haeghen YV, Naeyaert JMAD, Lemahieu I. An imaging system with calibrated color image acquisition for use in dermatology. *IEEE Trans Med Imaging* 2000; **19**:722–730.

21 Grana C, Pellacani G, Cucchiara R, Seidenari S. A new algorithm for border description of polarized light surface microscopic images of pigmented skin lesions. *IEEE Trans Med Imaging* 2003; **22**:959–964.

22 Hanley JA, McNeil BJ. The meaning and use of the area under a receiver operating characteristic (ROC) curve. *Radiology* 1982; **143**: 29–36.

23 McKie RM, Fleming C, McMahon AD, Jarrett P. The use of the dermatoscope to identify early melanoma using the three-color test. *Br J Dermatol* 2002; **146**:481–484.

24 Steiner A, Binder M, Schemper M, Wolff K, Pehamberger H. Statistical evaluation of epiluminescence microscopy criteria for melanocytic pigmented skin lesions. *J Am Acad Dermatol* 1993; **29**:581–588.

25 Pehamberger H, Binder M, Steiner A, Wolff K. Early recognition and prognostic markers of melanoma. *Melanoma Res* 1993; **3**: 279–284.

26 Soyer HP, Smolle J, Leitinger G, Rieger E, Kerl H. Diagnostic reliability of dermoscopic criteria for detecting malignant melanoma. *Dermatology* 1995; **190**:25–30.

27 Nachbar F, Stolz W, Merkle T, Cognetta AB, Vogt T, Landthaler M, *et al.* The ABCD rule of dermatoscopy. *J Am Acad Dermatol* 1994; **30**: 551–559.

28 Menzies SW, Ingvar C, McCarthy WH. A sensitivity and specificity analysis of the surface microscopy features of invasive melanoma. *Melanoma Res* 1996; **6**:55–62.

29 Argenziano G, Fabbrocini G, Carli P, De Giorgi V, Sammarco E, Delfino M. Epiluminescence microscopy for the diagnosis of doubtful melanocytic skin lesions. Comparison of the ABCD rule of dermoscopy and a new 7-point checklist based on pattern analysis. *Arch Dermatol* 1998; **134**:1563–1570.

30 Braun RP, Rabinovitz H, Oliviero M, Kopf A, Saurat JH. Pattern analysis: a two-step procedure for the dermoscopic diagnosis of melanoma. *Clin Dermatol* 2002; **20**:236–239.

31 Seidenari S, Burroni M, Dell'Eva G, Pepe P, Belletti B. Computerized evaluation of pigmented skin lesion images recorded by a videomicroscope: comparison between polarizing mode observation and oil/slide mode observation. *Skin Res Technol* 1995; **1**:187–191.

32 Pellacani G, Seidenari S. Comparison between morphological parameters in pigmented skin lesion images acquired by means of epiluminescence surface microscopy and polarized-light videomicroscopy. *Clin Dermatol* 2002; **20**:222–227.